CLM-P833

CLM-P833

A phenomenological interpretation of trace impurity transport

F.A. Haas
A. Thyagaraja

UK ATOMIC ENERGY AUTHORITY

Culham Laboratory

CLM-P833

A phenomenological interpretation of trace impurity transport

F.A.Haas and A.Thyagaraja

Culham Laboratory, Abingdon, Oxfordshire OX14 3DB, UK
(EURATOM/UKAEA Fusion Association)

Abstract

An interpretive theory of trace impurity transport in tokamaks is presented. It is based on an earlier phenomenological approach developed by the authors for describing tokamak plasma transport experiments. The present model is used to explain disparate phenomena observed in ALCATOR C and DITE in a unified framework. Predictive numerical calculations are presented for DITE conditions. If experimentally confirmed, the model could be used to correlate plasma properties with trace impurity behaviour.

January, 1988

1. INTRODUCTION

Although many groups have investigated trace impurity transport, the results tend to be diverse, complex and sometimes contradictory. The objective of the present paper is to provide a possible theoretical interpretation of this area of study. In order to keep our discussion within bounds we shall only consider the recent experiments on DITE (AXON et al (1987), HAWKES et al (1987)) and those on ALCATOR C (MARMAR et al (1982)). These are contrasting experiments and therefore a good test of our interpretation. There is no reason to believe, however, that the interpretation presented here could not describe results obtained in other experiments. Since the background plasma transport in tokamaks is well-known to be anomalous, we shall also consider the possible relationship between this phenomenon and the transport of trace impurities.

Most of the ALCATOR C results obtained by MARMAR et al (1982) were interpreted by them in terms of an anomalous impurity particle diffusivity. Recent DITE results, on the other hand, present a more complex picture. For the same values of plasma density and other parameters, two different confinement regimes have been observed in DITE for a given impurity species. The only identifiable difference in experimental conditions between the two regimes is the presence or otherwise of gas-puffing, and consequently, the difference in values of $\frac{d\bar{n}_e}{dt}$. The essence of our interpretation consists of the following: we show in effect, that if the impurity flux is regarded as the sum of a Pfirsch-Schluter flux and an anomalous flux, the results of ALCATOR and DITE are interpretable in a simple unified way and the scalings with background mass and impurity charge can be derived. We remark that MARMAR et al (1982) have previously suggested fluxes of this type. In the present paper, however, we have developed this suggestion and shown how diverse results can be fitted into a unified phenomenological framework.

2. BACKGROUND PLASMA TRANSPORT.

For clarity, we begin by summarising our earlier phenomenological work (HAAS and THYAGARAJA, 1986) on the transport properties of the background plasma. In this we considered a single temperature model in which $T_e = T_i$ and radiative losses were taken as negligible as compared with anomalous thermal conduction. We investigated only those processes which occur on a time-scale comparable with the election energy confinement time; on this slow time scale all inertial effects are neglected. Restricting ourselves to cylindrical geometry,* we consider the variables $n(r,t)$, $T_e(r,t)$, $v_r(r,t)$, $p(r,t)$, $B_\theta(r,t)$ and $B_\phi(r,t)$. Given sources and appropriate boundary conditions, these variables are determined from the equations below. Thus the continuity equation is

$$\frac{\partial n}{\partial t} + \frac{1}{r}\frac{\partial}{\partial r}(rnv_r) = S_p(r,t), \tag{1}$$

with the energy equation written as

$$\frac{3n}{2}\left\{\frac{\partial T_e}{\partial t} + v_r\frac{\partial T_e}{\partial r}\right\} + nT_e\frac{1}{r}\frac{\partial}{\partial r}(rV_r)$$

$$= \frac{1}{r}\frac{\partial}{\partial r}\left(rn\chi_{\perp e}\frac{\partial T_e}{\partial r}\right) + \eta_\phi j_\phi^2 + \eta_\theta j_\theta^2 + P_{aux}(r,t). \tag{2}$$

The equation of state is

$$p = 2nT_e, \tag{3}$$

---

* For ease of comparison with later formulae, the cylindrical co-ordinate "z" is re-labelled "ϕ". Thus, $B_\phi \equiv B_z$ for example.

with the radial momentum balance

$$\frac{\partial p}{\partial r} = \frac{1}{c} (j_\theta B_\phi - j_\phi B_\theta) \tag{4}$$

The toroidal and poloidal components of Ampere's equation are

$$\frac{4\pi}{c} j_\phi = \frac{1}{r} \frac{\partial}{\partial r} (rB_\theta) \tag{5}$$

and

$$\frac{4\pi}{c} j_\theta = -\frac{\partial B_\phi}{\partial r} \tag{6}$$

The poloidal and toroidal components of Ohm's law are given by

$$-\frac{V_r B_\phi}{c} = \eta_\theta j_\theta \tag{7}$$

and

$$-\frac{1}{c} \frac{\partial A_\phi}{\partial t} + \frac{V_r B_\theta}{c} + E_{ext}(t) = \eta_\phi j_\phi, \tag{8}$$

with the vector potential $\underline{A}$ related to $\underline{B}$ through

$$B_\phi = \frac{1}{r} \frac{\partial}{\partial r} (rA_\theta) \tag{9}$$

and

$$B_\theta = -\frac{\partial A_\phi}{\partial r} \tag{10}$$

The main difference between this model and many earlier 1 - D or 3/2 - D models of transport in Tokamaks is the explicit and crucial use of the pressure-balance and poloidal - Ohm's law. In our previous paper we showed that this extra coupling had important consequences in both the steady-state and its time evolution.

It was pointed out by BICKERTON(1978) that for the law of conservation of momentum for electrons and ions to be compatible with the observed form and magnitude of the radial particle flux, the poloidal resistivity η_θ must be of order 100 times the Spitzer value. In our own paper we demonstrated that if the poloidal field and particle transport rates are to be comparable - as is generally believed - then $\eta_\theta = c_1 \eta_\phi B^2_\phi / B^2_\theta$ where c_1 is a constant of order unity. In other words, η_θ is required to be anomalously large as compared with Spitzer. With this assumption, taking the electron thermal diffusivity $\chi_{\perp e}$ to have a typically "anomalous" value and adopting appropriate boundary conditions and sources, we were able to interpret a range of phenomena. Thus, for example, we were able to interpret the density-clamp in DITE, behaviour of the Hugill diagram, and some of the principal features of the L-H transition in ASDEX. We were also able to show the existence of transport mechanisms which may limit density and poloidal-beta independently of radiative, MHD or gross-disruptive processes.

Given the previous success of this model, we propose to use it to establish the plasma profiles of $n(r,t)$ and $T_e(r,t)$ through which the trace impurities are transported.

3. THE IMPURITY EVOLUTION EQUATION

The results relating to the recent DITE work (AXON et al, HAWKES et al (1987)) are shown in Fig. 1. This pertains to a 100 kA, 2.6 T discharge with a graphite limiter of 0.21m.

Non-recycling aluminium was injected into the plasma by laser-ablation. In the figure the solid points refer to $\frac{d\bar{n}_e}{dt} \sim 0$ (constant density), while the open points correspond to $\frac{d\bar{n}_e}{dt} > 10^{19} m^{-3} s^{-1}$, for a range of values of electron density at the time of impurity injection. In this context, impurity "confinement time", τ_{imp}, refers to the exponential decay time

of the time-dependent brightness profile as measured by experiment. At low density there is no difference, within experimental errors, between the impurity confinement in constant and rising density discharges. For constant density, the confinement time increases with density up to the electron highest density achieved. In contrast, discharges with $\frac{d\bar{n}_e}{dt} > 0$ show a clear maximum confinement time, then a decrease with density.

We now demonstrate an interesting property of the impurity transport equation. We assume that in cylindrical geometry the impurity density $n_I(r,t)$ evolves according to the equation

$$\frac{\partial n}{\partial t} I = - \frac{1}{r} \frac{\partial}{\partial r} \left(r \Gamma_I(r,t) \right) \tag{11}$$

with $\Gamma_I(r,t)$ defined to be

$$\Gamma_I(r,t) \equiv - D_I \frac{\partial n_I}{\partial r} - U_I n_I \ . \tag{12}$$

In Eq.(12), D_I corresponds to a perpendicular impurity diffusion coefficient while U_I represents an inward impurity convection (for positive U_I). In practice, D_I and U_I are functions of position and time, dependent on plasma properties but not on n_I. Thus given D_I, U_I and initial and boundary conditions, then $n_I(r,t)$ can be determined. To explain the results in the simplest possible terms, we make the assumption

$$\left.\begin{aligned} D_I &= D_a \, f_D \, (r/a) \\ U_I &= U_a \, f_U(r/a), \end{aligned}\right\} \tag{13}$$

where f_D and f_U are positive profile functions with the property $f_D(1) = f_U(1) = 1$; $f_D(0) = f_U(0) = 0$ and both functions can be

arbitrary, apart from the fact they are taken to be increasing with r/a. D_a is a positive parameter having the dimension of a diffusivity, while U_a can be positive or negative and has the dimensions of a velocity. It is useful to define a convection parameter $C_a \equiv a \frac{U_a}{D_a}$ and a characteristic time $\tau_{diff} = a^2/D_a$. The boundary conditions for n_I are $n_I(a,t) = 0$ and $\Gamma_I(o,t) = 0$. Keeping the initial and boundary conditions fixed, we solve the above equation numerically for different values of C_a and τ_{diff}. In order to represent the laser-ablation experiment the initial conditions for n_I are specified as follows: $n_I(r,o) = 0$ for $r/a < 0.8$, $n_I(r,o) = 10$ for $0.8 < r/a < 0.9$, and $n_I = 100(1.0 - r/a)$ for $r/a > 0.9$. This choice adequately represents the experimental condition that at $t = 0$ the impurity is concentrated near the edge of the plasma. It should be stressed that our results are not sensitively dependent on the precise forms for f_D and f_U, and the choice of initial conditions.

It follows directly from Eq.(11) that the total number of impurities

$$N_{tot}(t) = \int_0^a r\, N_I(r,t)dr \qquad (14)$$

decreases monotonically with time. To proceed, we make certain specific choices for f_D and f_U - these will be justified later in the paper. Defining the line-average through the central chord to be

$$\bar{N}(t) = \int_0^a n_I(r,t)dr, \qquad (15)$$

we find this quantity to show a sharp rise followed by an exponential fall from the maximum, as shown in Fig.2. This corresponds to the behaviour of the experimentally obtained brightness function, although of course $\bar{N}$ is not necessarily a direct measure of the brightness. Fig.2 is easy to interpret, especially for positive values of C_a. For early times (first one or two milliseconds after injection at t=0), Γ_I is totally inward, both the D_I and U_I terms going in the same direction - the inward

penetration phase. As Fig.3 shows, once a central bell-shaped profile is established (corresponding to maximum $\bar{N}$), the profile decays exponentially in a rather self-similar fashion. The characteristic exponential decay time of $\bar{N}$ can be obtained numerically and is denoted by τ_{rel} (in order not to confuse it with the experimentally measured τ_{imp}). It is apparent from dimensional arguments that the non-dimensional ratios $\frac{\tau_{rel}}{\tau_{diff}}$ and C_a are functionally connected by a universal relationship once f_D and f_U are specified. This is illustrated in Fig. 4, which shows a remarkable "transitional" behaviour.

Thus for $C_a \lesssim 8.0$, τ_{rel}(decay time of $\bar{N}$) is of order τ_{diff}($= a^2/D_a$). In the neighbourhood of $C_a \sim 14$, however, $\frac{\tau_{rel}}{\tau_{diff}}$ is of order 100. It should be noted that this sensitivity is essentially independent of our specific choices for f_D, f_u; any reasonable positive profile functions will lead to roughly the same result. It is possible that the two impurity confinement times (τ_{imp}) demonstrated by DITE are an indication of this property of the transport equation. Experimentally, C_a could change due to variations in $\frac{d\bar{n}_e}{dt}$ modifying both D_a and U_a. Since τ_{diff} is smoothly varying with D_a, τ_{rel} can apparently exhibit dramatic changes if the C_a of the experiment happens to be in the "transitional" range $C_a \sim 10.0$. Thus without seeking a detailed link between plasma properties on the one hand and D_a, U_a, f_U and f_D on the other, we can account for the observations in DITE as being due to fairly modest changes in the experimental conditions. This interpretation suggests that ALCATOR possibly corresponds to $C_a \sim 1.0$, while purely neoclassical expressions for D_a and U_a would lead to $C_a >> 10.0$.

We note that the assumptions of HAWKES et al correspond to $f_D \equiv 1$, $f_U = r/a$. Their S is $C_a/2$ in our notation. They have empirically fitted their observed decay time by the expression

$$\tau = 0.173 \frac{a^2}{D} \exp(- 0.34S).$$

It is clear that the minus sign is a typographical error since τ must increase with S. As our numerical calculation shows, there should also be an S^{α} term multiplying the exponential. However, for limited ranges of S, the exponential form alone probably captures the essence of the scaling.

4. PHENOMENOLOGICAL IMPURITY TRANSPORT COEFFICIENTS.

We now consider the possible physical bases of the coefficients D_I and U_I. We shall assume that D_I and U_I may be written as

$$D_I = D_I^{PS} + D_I^{Anom}, \quad U_I = U_I^{PS} + U_I^{Anom} \tag{16}$$

where the superfixes PS and Anom refer to Pfirsch-Schluter and anomalous, respectively. Following the literature (see RUTHERFORD (1974) for example), the appropriate forms for the Pfirsch-Schluter parts of D_I and U, are as given below:

$$D_I^{PS} = (1 + 2q^2) \frac{\rho_i^2 n_i Z_i^2}{n_I \tau_{iI} Z_I^2} \tag{17}$$

where

$$\rho_i^2 = \frac{T_i m_i c^2}{Z_i^2 e^2 B_{\phi 0}^2}, \qquad \tau_{iI} = \frac{3 m_i^{1/2} T_i^{3/2}}{4(2\pi)^{1/2} n_I Z_I^2 e^4 \ln \Lambda_{iI} Z_i^2} \tag{18}$$

and

$$U_I^{PS} = D_I^{PS} \left\{ \frac{1}{T_i} \frac{dT_i}{dr} - \frac{Z_I}{Z_i p_i} \frac{dp_i}{dr} \right\} \tag{19}$$

These results have been derived on the basis of concentric circular flux - surfaces radius, r, and the suffices i and I denote the background

plasma ions and impurity ions, respectively. It is further assumed that $T_i = T_e = T_I$ and $n_e = Z_i n_i$. we have also neglected thermal force terms. Although these terms can contribute, they are not expected to produce any significant qualitative changes to the final results. It should be noted that the first term in the bracket $(1+2q^2)$ which occurs in D^{PS}, represents the cylindrical (or classical) contribution, which arises in the limit $a/R \to 0$.

We now turn to a discussion of the anomalous parts of U_I and D_I. In discussing U_I^{Anom} we reconsider the cylindrical/classical calculation of the radial impurity velocity V_{Ir}. We are particularly concerned with the contribution which is due to collisions with the electrons. Although this would normally be expected to be small - for reasons which will become apparent later - the impurity - electron collisions can be important. Thus, it can be shown that V_{Ir} due to this interaction is given by

$$V_{Ir} = - \frac{c}{e^2 B_\phi Z_I n_I} \cdot \frac{m_e}{\tau_{eI}} j_\theta \cdot \tag{20}$$

For classical collisions

$$\tau_{eI} = \frac{n_i}{n_I} \frac{Z_i^2}{Z_I^2} \frac{\ell n \Lambda_{ei}}{\ell n \Lambda_{eI}} \tau_{ei}, \tag{21}$$

where $$\tau_{ei} = \frac{3 m_e^{1/2} T_e^{3/2}}{4(2\pi)^{1/2} n_e Z_i e^4 \ell n \Lambda_{ei}} \tag{22}$$

It is straightforward to write V_{Ir} in the form

$$V_{Ir} = - \frac{2c}{n_I B_\phi} \eta_{class} j_\theta \frac{Z_I}{Z_i^2} \frac{\ell n \Lambda_{eI}}{\ell n \Lambda_{ei}} \tag{23}$$

$$\text{with } \eta_{class} = \frac{m_e}{2e^2 n_e \tau_{ei}} . \qquad (24)$$

Now in our background plasma transport studies we showed that the electron-ion interaction in the poloidal direction is anomalous. More specifically, in this direction η_{class} should be replaced by η_θ, where $\eta_\theta \sim \eta_{class} B_\phi^2/B_\theta^2$. We now assume that the electrons also interact anomalously with the impurities in the poloidal direction. That is, the electrons do not distinguish between plasma ions and impurity ions in their interactions. Carrying out this replacement, and substituting for j_θ from pressure-balance, we finally obtain

$$U_I^{Anom} = \frac{C^2}{2B_\phi^2}\,\eta_\theta \cdot \frac{Z_I}{z_i^2}\,\frac{\ell n \Lambda_{eI}}{\ell n \Lambda_{ei}}\,\left(\frac{dp}{dr} + \frac{j_\phi B_\theta}{C}\right). \qquad (25)$$

We shall show later that there are circumstances when U_I^{Anom} is dependent on the pressure balance. Thus, U_I^{Anom} is negative (implying outward convection) if $\frac{dp}{dr} + \frac{j_\phi B_\theta}{C} < 0$. Interestingly, due to cancellations, there is no equivalent contribution arising from the Pfirsch-Schluter terms.

In the earlier work of COPPI and SHARKEY (1981), it was found that experimental observation could be reasonably interpreted if the anomalous plasma diffusivity D_{plasma}^{Anom} was assumed to be of the order of the anomalous electron thermal diffusivity $\chi_{\perp e}$. As described in Section 2 we have made the same assumption in our own more recent phenomenological work (HAAS and THYAGARAJA (1986)) concerning plasma transport. Analogously we make the heuristic assumption that the anomalous impurity diffusivity D_I^{Anom} is also of order the anomalous electron thermal diffusivity $\chi_{\perp e}$. This hypothesis is based on the idea that the turbulent diffusion flux of the impurity ions is of the same order as the plasma ions and electrons. This would be the case, for example, if D_I^{anom} is due to the fluctuating

$\underline{E} \times \underline{B}$ drift, that is, independent of species mass and charge. At the present time, there is no conclusive experimental proof of this assumption.

We now take $D_I^{Anom} = D_a f_D(r/a)$, where the function $f_D(r/a)$ is chosen to be equal to the profile of $\chi_{\perp e}$, which is itself taken to have the Gruber form $K/n_e T_e^{1/2}$, K being a constant; for DITE conditions D_I^{PS} is unimportant. We further require the background density and temperature profiles, n_e and T_e. These are evolved using the equations described earlier in Section 2.

Assuming DITE ohmic conditions the n_e and T_e profiles were evolved for some 400 ms, at which time a steady-state had been established. The impurity evolution equation itself, Eq.(1), is solved in the subsequent 100 ms subject to the stated initial and boundary conditions, using the steady n_e and T_e profiles prevailing at this time. The impurity evolution, of course, has no influence on the plasma equilibrium and transport. Keeping U_a fixed as given by Eqs.(7), (8) and (9), we have varied D_a over the range of interest to get different values of C_a, as shown in Fig.4. The value of the confinement time τ_{diff} ranges from 0.5 to 50 ms. Thus over this range for values of C_a from about 1.0 to 15.0, D_I^{anom} is of the same order as D_{plasma}^{anom} and χ_e.

5. SCALING RESULTS AND COMPARISON WITH ALCATOR DATA

We have considered the scalings of τ_{rel} with respect to various parameters for ALCATOR reported in Marmar et al. In contrast to DITE, the conditions in ALCATOR C considered are precisely in the range where the Gruber scaling with n_e is not valid. The choice for D_I^{anom} could be made specific if the data relating to $\chi_{\perp e}$ were known. In Marmar et al. they take D^{anom} to be simply a constant ($3 \times 10^3 cm^2 s^{-1}$).

We follow a very similar procedure except that we take

$D_I^{anom} = \chi_{\perp e}$, where $\chi_{\perp e}$ is independent of n_e and chosen so as to give the correct electron energy confinement time (of order 10.0-20.0 ms) taken from PARKER et al (1985). Furthermore, D_I^{PS}, U_I^{PS} and U_I^{anom} are given by Eqns (17),(18),(19) and (25), with $\eta_\theta = \eta_{class} \frac{B_\phi^2}{B_\theta^2}$. For a set of typical conditions, we consider the variation of τ_{rel} with the mean density $\bar{n}_e$ over the range $10^{14} cm^{-3}$ to $5.0 \times 10^{14} cm^{-3}$. Fig.(5) reproduces the experimental results of MARMAR ET AL (1982) and our calculations. The calculated values show that the S_i relaxation time is weakly increasing with mean density and is in reasonable agreement with experiment. Thus for the ALCATOR conditions Eq(11), together with the assumptions for D_I and U_I stated above, show τ_{rel} to depend only weakly on $\bar{n}_e$. This result is clearly related to the fact that D_I^{anom} is independent of $\bar{n}_e$ for the present conditions and that U_I (although dependent on $\bar{n}$), exerts much less influence on τ_{rel} than D_I^{anom}, indicating that in ALCATOR, C_a is less than 10.0. In fact, if τ_{rel} were to be plotted against τ_{Ee}, as given by PARKER et al (1985), (instead of $\bar{n}_e$) we should obtain a straight line, indicating a proportionality of these two confinement times.

We now consider a more general study of the expected scalings. It is essential to recognise that the results of Marmar et al pertain to two different density ranges. In the low density range $\bar{n}_e$ = 1.0 to 2.0×10^{14}, $\chi_{\perp e}$ and τ_{Ee} have a significant density dependence. Our assumption $D_I^{anom} = \chi_{\perp e}$ is effectively equivalent to the statement $\tau_{diff} \tilde{\tau}_{Ee}$, where τ_{diff} is defined as before. In the higher density range $\bar{n} = 2.0 \times 10^{14}$ to 6×10^{14}, $\chi_{\perp e}$ is essentially saturated as shown by PARKER et al. The scalings considered above were appropriate to this higher range. We now derive the scalings of τ_{rel} relative to τ_{diff} from our equations. The scalings of τ_{rel} by itself can then be deduced by inserting the experimentally obtained scaling of τ_{diff}. Our

studies suggest that experimental results on impurity transport are most easily understood in terms of the ratio of the impurity relaxation time to the background electron energy confinement time. Neglecting D_I^{PS} we consider the two non-dimensional ratios, $a\,\dfrac{U_I^{PS}}{D_I^{anom}} \equiv a\dfrac{U_I^{PS}}{\chi_{\perp e}}$ and $\dfrac{U_I^{anom}}{U_I^{PS}}$. Thus

$$a\,\frac{U_I^{PS}}{\chi_{\perp e}} \sim \frac{D_I^{PS}}{\chi_{\perp e}}\,\frac{Z_I}{Z_i} \sim \frac{q^2 n_e m_i^{1/2} c^2 e^2}{B_\phi^2 T_i^{1/2} \chi_{\perp e}} \cdot Z_I \qquad (26)$$

We now consider $U_I^{anom}/\,U_I^{PS}$. This quantity is

$$\lesssim \frac{(U_I^{anom})_{max}}{U_I^{PS}} \simeq \left(\frac{m_e}{m_i}\right)^{1/2} \frac{1}{Z_i} \left(\frac{R}{a}\right)^2 \qquad (27)$$

We note first of all from Eq(27) that U_I^{anom}, at its strongest, is of order U_I^{PS}. It is interesting to observe that the effect of U_I^{anom} relative to U_I^{PS} decreases as the background mass increases and also with the background charge. Interestingly, both U_I^{PS} and U_I^{anom} are linearly proportional to Z_I and hence the impurity charge does not affect their ratio. When we are discussing situations in which the background plasma is in a quasi-stationary state and the impurity evolution takes place against this background, it seems reasonable to regard U_I^{anom} as providing a small correction to U_I^{PS}. Turning our attention to Eq. (26), we remark that under the assumptions of our phenomenological picture for Ohmic conditions, where $\chi_{\perp e}$ is represented by Gruber scaling, we have $I_p^2 \propto nT_e$. Thus we expect the combination

$\dfrac{q^2 n_e}{B_\phi^2 T_i^{1/2} \chi_{\perp e}}$ to be independent of n, T_e, I_p and B_ϕ. Hence the ratio

$$\frac{aU_I^{PS}}{\chi_{\perp e}} \equiv C_a \propto m_i^{1/2} Z_I \qquad (28)$$

As we have seen τ_{rel}/τ_{Ee} is "universally" determined by C_a. This suggests that under the conditions stated, τ_{rel}/τ_{Ee} is purely a function of the background mass and the impurity charge. If the numerical value of C_a is $\lesssim 10.0$, we can write $\tau_{rel}/\tau_{Ee} \propto m_i^{1/2} Z_I$. If C_a is $\gtrsim 10.0$ the functional dependence is not linear, but could be much stronger. Under such conditions it would be very difficult to distinguish τ_{rel} from the purely neoclassical confinement time. In any event, our theory shows that it must be much greater than the electron energy confinement time.

It is of interest to note that even in the high density regime where $\chi_{\perp e}$ is taken to be a constant independent of n_e, we get the same scaling with $m_i^{1/2}$ and Z_I, but for a different reason. In the absence of strong radial flows, $nT \propto I_p^2$, and if $\chi_{\perp e}$ is independent of n, T_e is independent of both n and I_p (saturated ohmic heating). Eq(15) then shows that C_a is proportional to $m_i^{1/2}$ and Z_I only.

We note that the linear dependence on Z_I in practice can be masked depending on the value of C_a. Thus the slope $\frac{\Delta\tau_{rel}}{\Delta Z_I}$ is a function of Ca. In fig. 9 of Marmar et al they found (for their conditions) that $\frac{\Delta\tau_I}{\Delta Z_I}$ is rather small implying that τ_I was not a strong function of Z_I. We have calculated τ_{rel} for Z_I varying between 12.0 to 24.0. $\frac{\Delta\tau_I}{\Delta Z_I}$ is of order 0.2 msec, namely, consistent with experiment. This corresponds to a value of C_a of order 8.0. For larger values of C_a, $\Delta\tau_I/\Delta Z_I$ can be much larger. This result shows the need for care in interpreting empirically derived scalings. It also shows the importance of impurity measurements, where m_i and Z_I are varied over as large a variation as possible.

We note that we do not get any simple relation between Z_i and τ_{rel} in our theory. In the ALCATOR low density regime it is observed that τ_{rel} and Z_{eff} (equivalent to Z_i) are apparently proportional to each other. As Marmar et al themselves point out, it is precisely this regime in which Z_{eff} and $\bar{n}_e$ are linearly related. In the absence of any data relating to variations of Z_{eff} at constant $\bar{n}_e$, the observed scaling could simply be a reflection of the relationship between τ_{rel}, τ_{Ee} and $\bar{n}_e$ at low density. The relationship of τ_{rel}/τ_{Ee} to the background ion mass is qualitatively consistent with experiment; that is τ_{rel} increases with $m_i^{1/2}$ τ_{Ee}. However, since the scaling of τ_{Ee} with m_i is not well-known, this remains a prediction to be confirmed by experiment. The other prediction of the theory is the clear absence of any dependence of τ_{rel} on the mass of the impurity species itself. Marmar et al give scalings with parameters such as R, a and q. It is very difficult to compare theory and experiment in these cases, for two reasons; (i) it is easiest to compare theoretical and empirical scalings when the latter are expressed in terms of the ratio τ_{rel}/τ_{Ee} (2) In deriving experimental scalings it is hard to be sure which parameters are held constant while others vary. For these reasons we have restricted ourselves to the above scalings.

6. THEORETICAL PREDICTIONS FOR DITE IMPURITY TRANSPORT

We now move on to a set of predictions for DITE conditions based on the above ideas. In all the cases considered we assume that the χ_{1e} obeys the Gruber scaling. This assumption itself could and should be tested to check the theory, and if need be modified. Bearing in mind the existing experiments in DITE (they show two different scalings for τ_{rel} with $\bar{n}_e$ distinguished by the differing values of $\frac{d\bar{n}_e}{dt}$), it would be interesting to repeat the experiments with identical plasma conditions but differing values of Z_i. If our theory is correct, the transition value of C_a and τ_{rel} itself, ought to depend on Z_i. It seems to us that

corresponding studies in H, D and He plasmas could be used to verify the mass-dependence of τ_{rel}. In the above work we have so far ignored the effects due to U^{anom} term. This can be most clearly seen in transient experiments in which the plasma is evolving while the impurity transport is taking place. There are two possibilities; in the first, which we shall call a 'temperature clamp', when the impurity is introduced into an ohmic plasma, an external RF source is switched on and the plasma is heated at constant density and current. Since the temperature and consequently the plasma pressure rises while the impurity density is evolving, we expect both the neoclassical and the U_I^{anom} terms to be affected by the temperature rise. This should therefore affect τ_{rel} and the time-dependence of the impurity brightness. Assuming χ_{le} is constant and $T_i \approx T_e$, our code can be used to calculate the changes and therefore provide an estimate of the U_I^{anom} term. The second (more complicated) possibility is a density clamp. In this case, the heat source is pure ohmic heating. At the time of impurity injection, neutral beam power is switched on and this both heats the plasma and adds particles. In earlier work we showed that the line average density is affected by the increased beam power (density clamp). We expect an analogous effect for the impurities through the U_I^{anom}.

We now present a number of simulations for DITE conditions. The purpose of these is to bring out certain qualitative predictions which the above theoretical interpretation makes. In no way are these results to be regarded as a detailed and comprehensive analytic theory of DITE experiments for the conditions stated.

The first of these simulations addresses the following question: given a typical DITE ohmic discharge, into which a trace impurity has been injected, what happens (if anything) with 1 MW of additional heating introduced into the plasma 100 ms after the impurity injection. To make things definite, we performed a numerical simulation assuming the following conditions:

$R_0 = 120$ cm , $a = 21.0$ cm , $B_{tor} = 2.6$ T ,

$I_p = 100$ kA , $\bar{n}_e$(ohmic state) $= 5.5 \times 10^{13}$,

$T_e = 0.6$ keV (ohmic), $Z_{eff} = 3.0$, $Z_I = 12.0$,

$m_i = 4.0\ m_p$, $q(a) = 4.8$, auxiliary heating power at 100 ms after impurity injection is 1 MW - kept constant for next 100 ms. No extra particle sources.

We find $\bar{n}_e = 2.5 \times 10^{13}/cm^3$ in the final state - 200 ms after impurity injection. Final $T_e = 1.7$ keV.

The results were obtained by solving the coupled plasma and impurity equations. For the plasma $\chi_{\perp e}$ was taken to have the Gruber scaling and maintained throughout 200 ms and thus no allowance was made for possible degradation due to auxiliary heating. The D_I^{anom} for the impurity is taken as $0.15\ \chi_{\perp e}$.

Fig.6a shows the evolution of the line average plasma density during 200-400 ms, ie during the impurity evolution. Fig.6b gives the evolution of the central temperature of the plasma for the same period. These two curves clearly show the effect of the 1 MW additional heat source without extra particle sources on the plasma properties. Thus T_e rises very sharply and quickly reaches its final value (in a time of order 25 ms), while the density is "clamped" and falls to roughly half its initial ohmic value.

The effect on the impurity line average density is shown in Fig.6c, whilst Fig.6d gives the behaviour of the impurity volume average density (equivalent to the total number of impurity particles within the plasma). Although these two curves are not exactly related to the impurity brightness curve, it is clear that the time variation of the brightness is simply related to them. It is also clear that in the ohmic phase the impurity evolution is an exponential decay except for the first few

milliseconds which are not shown. At the onset of heating it is clearly seen that a sharp increase in the decay rate occurs. In our particular example this reduction in impurity confinement time due to additional heating can be traced to three causes. For the reasons discussed already, the temperature rise and the density clamp in the plasma tend to make U_I^{PS} more outward than in the ohmic phase. Secondly, the net pressure increase due to power injection drives the U_I^{anom} term outward. Finally, D_I^{anom} tends to rise due to the fall in plasma density. Fig.7 shows the effect of heating on the impurity density profile evolution. Thus, it is clear from this figure, that the impurity density profile is much less peaked during the injection phase relative to the ohmic phase. Of course, the central impurity density falls sharply. From the point-of-view of impurity evolution, changes in the plasma properties produced by auxiliary heating tend to lower the value of the convection parameter $C_a = aU_I/D_I$ relative to the ohmic conditions. This translates itself into a much higher decay rate. We have conducted further studies to examine what happens if D_I^{anom} does not have the Gruber scaling with plasma density but remains constant in magnitude throughout the run. We have found that the qualitative behaviour is unaltered, although of course the reduction in the confinement time is somewhat less (since, in this case, it is entirely due to changes in U_I). In order to examine the roles of U_I^{PS} and U_I^{anom}, we have conducted further numerical experiments, which lead to the following two conclusions.

(1) In the ohmic state, U_I^{anom} is negligible compared to U_I^{PS}.
(2) However, with auxiliary heating the degradation in impurity confinement is due roughly in equal parts to U_I^{PS} and U_I^{anom}, suggesting that at higher power levels and temperatures, U_I^{anom} has an important role to play. Experiments conducted under the conditions similar to numerical simulations can therefore provide considerable insight both into the precise relationship between D_I^{anom} and $\chi_{\perp e}$ on the one hand, and in the scaling with plasma density and temperature of D_I^{anom} itself. In any event, our proposed interpretation predicts (other

things being equal) a degradation of impurity confinement with auxiliary heating, especially in the absence of particle sources due to the heating. It would be interesting to check this prediction against an experiment.

In Fig.8 we plot the results obtained under ohmic conditions varying only the background ion mass. The impurity confinement time (τ_{rel}) is clearly seen to be proportional to $(m_i)^{1/2}$ in accordance with Eq.(17). It must be remembered, that if τ_{rel}/τ_{diff} is plotted, one would get this result, irrespective of how $\tau_{diff} \sim (a^2/D_I^{anom})$ itself scaled with m_i. If our hypothesis that τ_{diff} and τ_{Ee} (electron energy confinement time) are simply related (by a factor independent of m_i), this prediction can be experimentally tested, although possibly not over as wide a range of m_i as in the numerical simulations.

In connection with the scaling of τ_{rel} with Z_I, we encounter a new result in contrast to the ALCATOR C conditions. Simple arguments suggest that τ_{rel} is proportional to Z_I; indeed in ALCATOR C the conditions suggest that the scaling is rather weak. Fig.9 shows a similar study for DITE for ohmic conditions in which the point $Z_I = 12$ is fiduciary in the sense that it corresponds to the ohmic state of Fig.6. In Fig.9 we have varied Z_I from 6.0 to 18.0 keeping all other conditions fixed. The effect on τ_{rel} is dramatic, and indeed, far from linear. This behaviour is reminiscent of the plot of τ_{rel}/τ_{diff} versus C_a presented earlier (Fig.1.), and may be thought of as a manifestation of the latter under realistic conditions. The reason for this apparently widely divergent behaviour in ALCATOR C and DITE, is the fact noted already: once C_a exceeds a value of about 8.0, the impurity diffusion equation predicts a very rapid increase in confinement time, making the result almost indistinguishable from Pfirsch-Schluter confinement. This difference in scaling cannot be predicted by simple dimensional arguments which were adequate in obtaining the $\sqrt{m_i}$ dependence. It seems to us that the Z_I scaling will provide a sensitive method for deducing the scaling of D_I^{anom}.

CONCLUSIONS.

We propose a model of trace impurity transport in tokamaks based on our earlier work on plasma transport. We show that the essential features of trace impurity transport experiments can be understood within this model. The different regimes of the experiments are related in our model to the interplay of the convective and diffusive terms in the radial impurity flux. For trace impurities with high Z the convective contributions are principally due to Coulomb collisions (in the Pfirsch-Schluter regime) with background ions. The diffusive contribution on the other hand appears to be dominated by anomalous processes. The effective diffusion coefficient for impurity ions is taken in our model to be simply related to the anomalous perpendicular electron thermal diffusivity. This hypothesis appears to be in reasonable qualitative and quantitative agreement with the available experimental data.

REFERENCES

AXON, K.B., et al (1987), Influence of Discharge Dynamics on Impurity Confinement in High density Ohmically Heated Tokamak Plasmas, to be published.

BICKERTON, R.J. (1978), J. Phys. D; Appl. Phys. II, 1781.

COPPI, B and SHARKEY, N. (1981), Nuclear Fusion 21, 1363.

HAAS, F.A. and THYAGARAJA, A (1986), Plasma Physics and Controlled Fusion, 28, No. 8, 1093.

HAWKES, et al (1987), 14th European Conference on Controlled Fusion and Plasma Physics, Madrid.

MARMAR, E.S., et al (1982), Nuclear Fusion, 22, No. 12, 1567.

PARKER, R.R., et al (1985), Nuclear Fusion 25, No. 9 1127.

RUTHERFORD, P.H. (1974), Phys of Fluids, 17, No. 9, 1782.

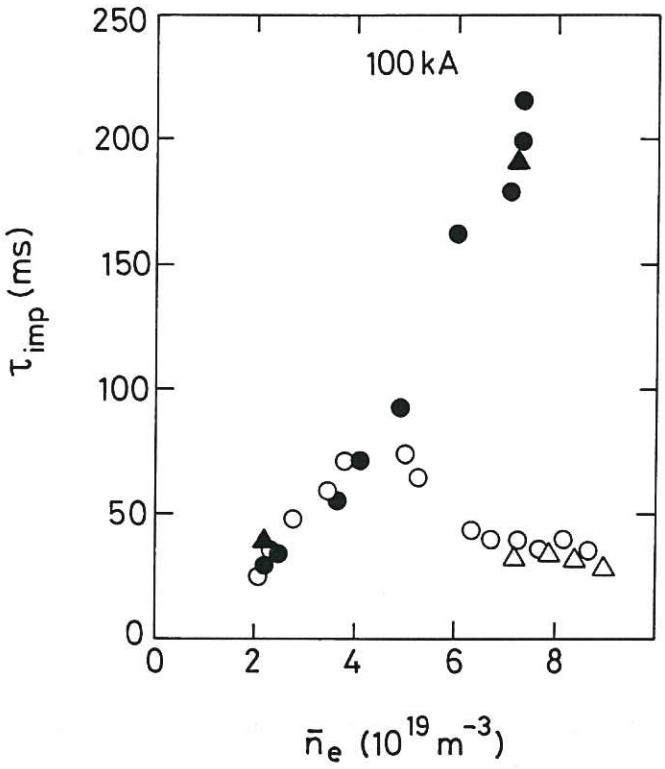

Fig.1. DITE experimental variation of impurity confinement with mean plasma density (reproduced from AXON et al). Open points rising density, solid points constant density, Δ indicate Aℓ XIII and circles are Aℓ XII.

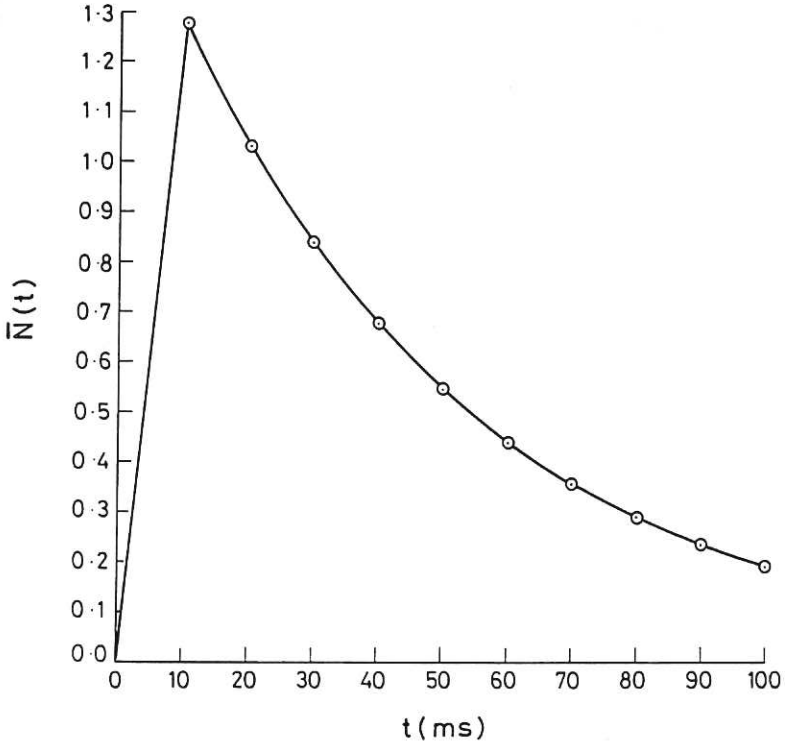

Fig.2. Typical calculated variation of $\bar{N}(t)$ with time for DITE conditions.

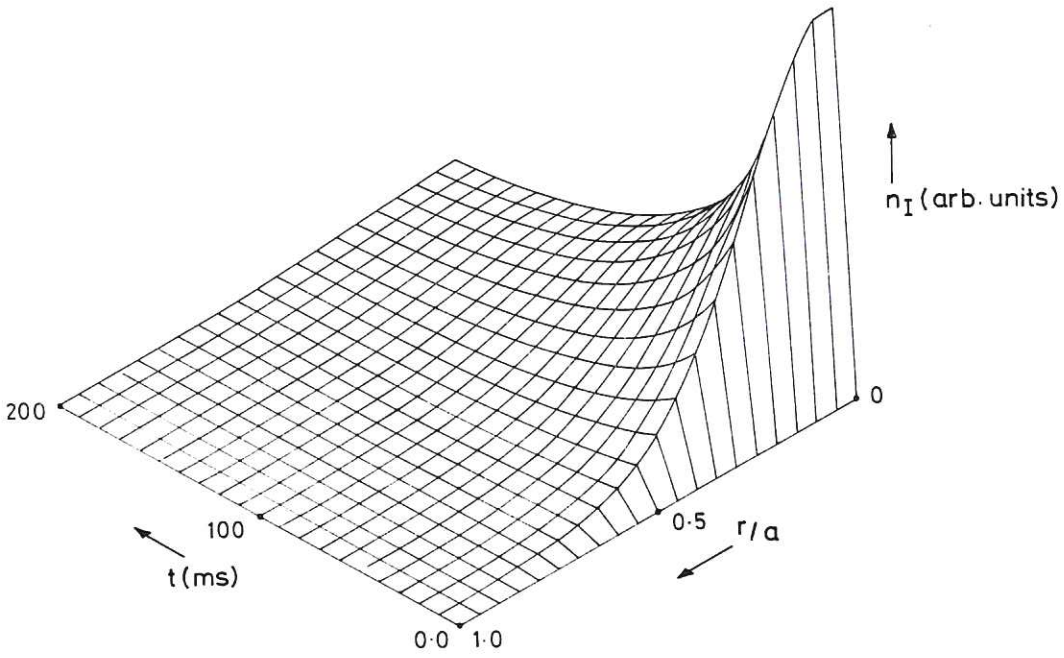

Fig.3. Calculated variation of the impurity profile surface for Ohmic DITE conditions corresponding to Fig.2.

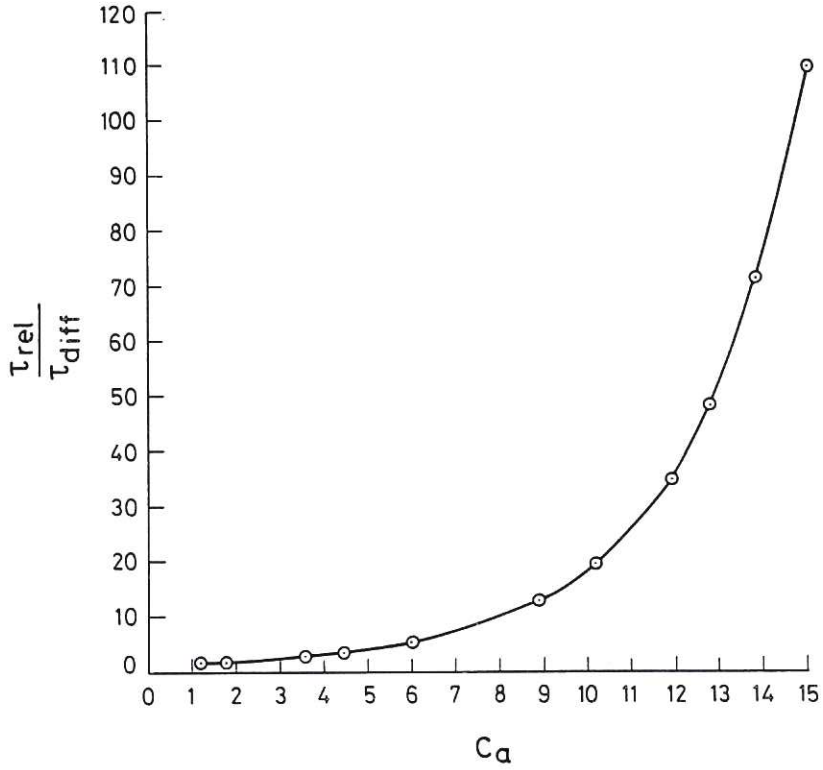

Fig.4. The calculated variation of τ_{rel}/τ_{diff} with the convection parameter C_a, keeping profiles and initial conditions fixed.

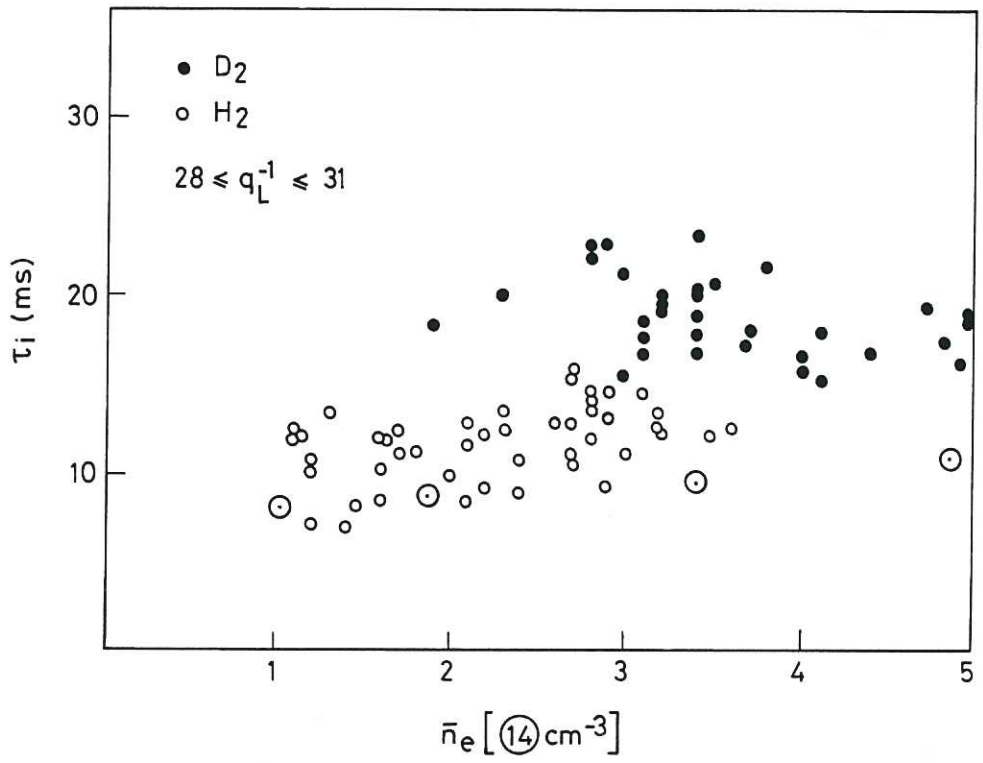

Fig.5. Silicon confinement time as a function of electron density. The experimental points for hydrogen shown by open circles, should be compared with the calculated points shown by ⊙. The experimental points are obtained from MARMAR et al.

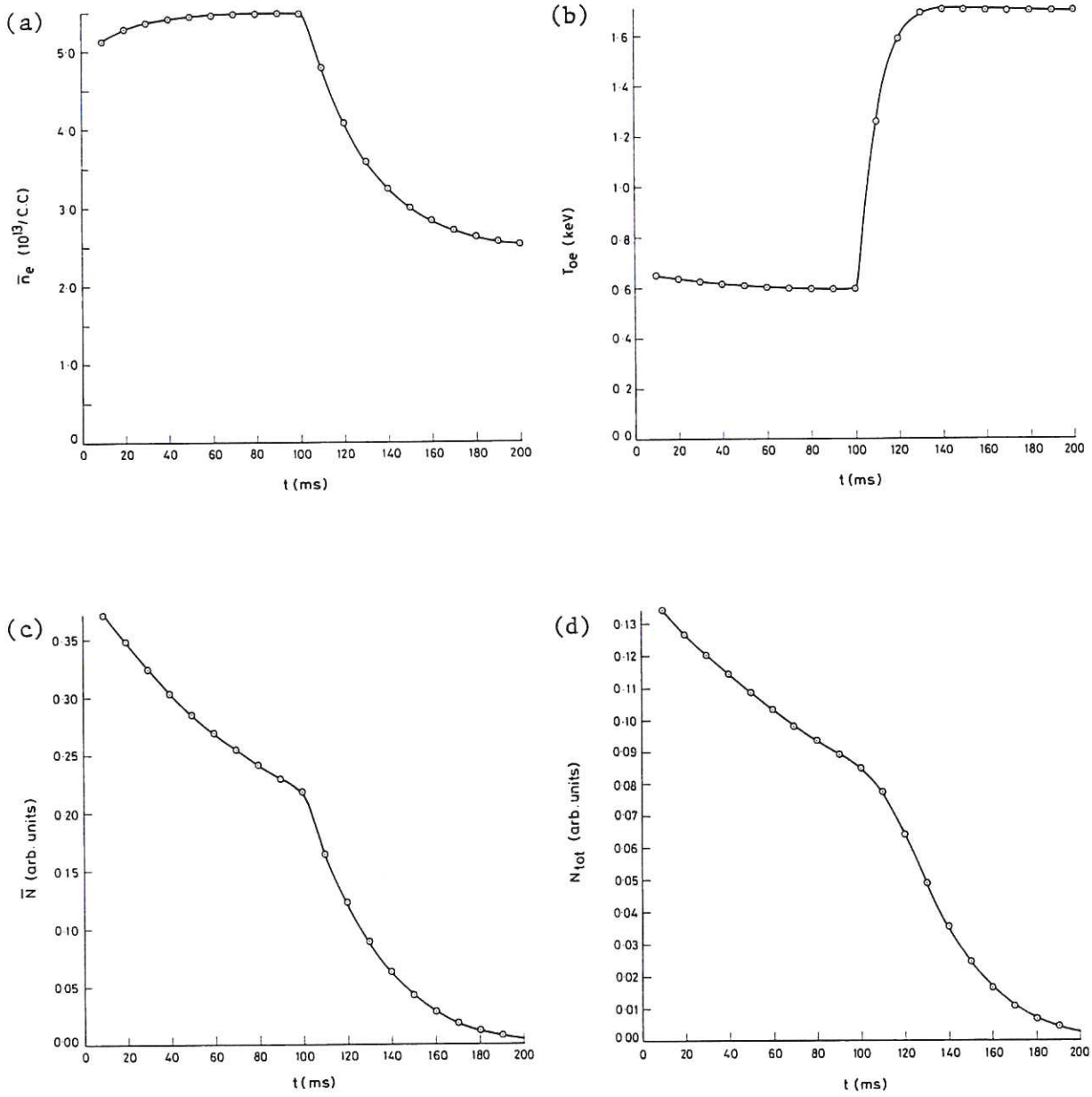

Fig.6. Time dependent profiles for the DITE temperature clamp simulation.

(a) Variation of mean electron density as a function of time.

(b) Variation of central electron temperature as a function of time.

(c) Variation of $\bar{N}$ as a function of time.

(d) Variation of N_{tot} as a function of time.

Note that t = 0 corresponds to the impurity injection during the ohmic phase, and, t = 100 ms corresponds to the time when the power source is switched on, with no extra particle source for the plasma and the impurities.

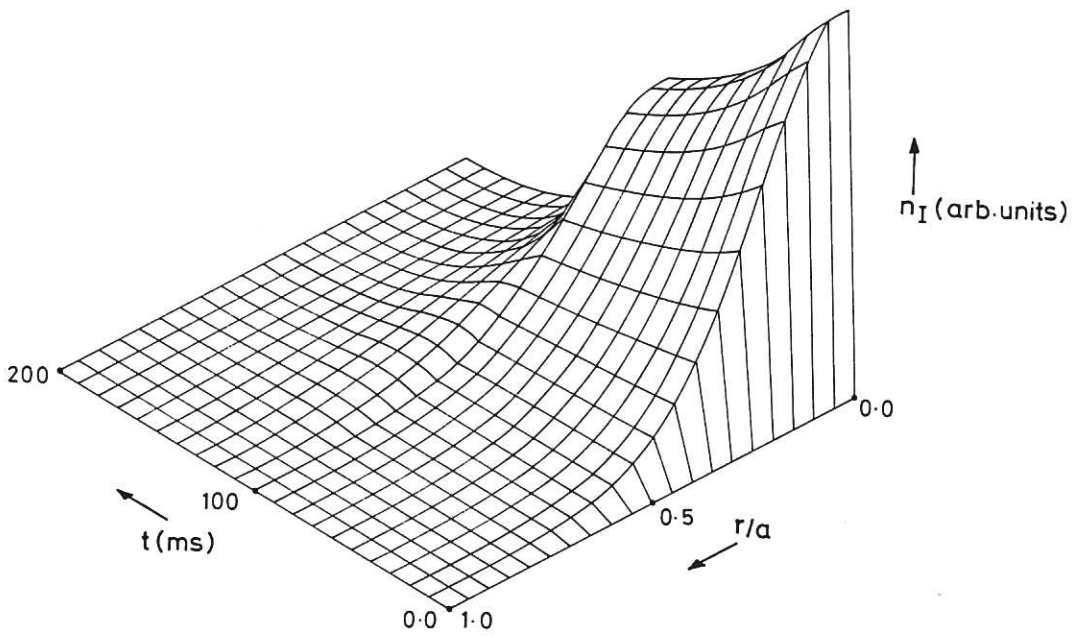

Fig.7. Evolution of the impurity profile surface during the DITE temperature clamp simulation, corresponding to Fig. 6.

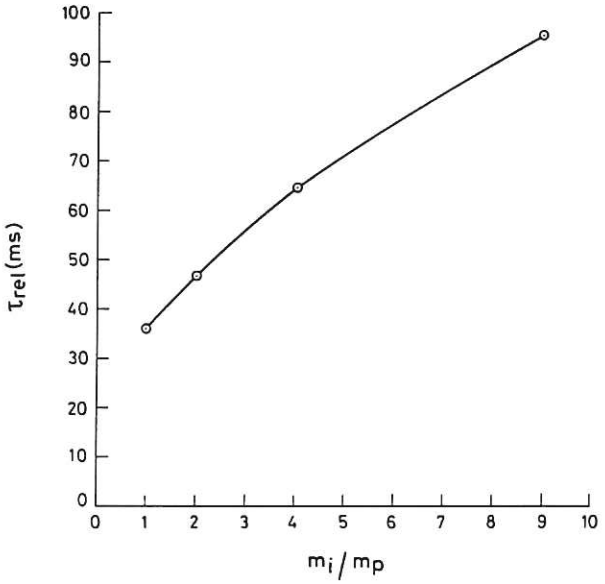

Fig.8. Scaling of τ_{rel} with background ion mass as predicted by the model.

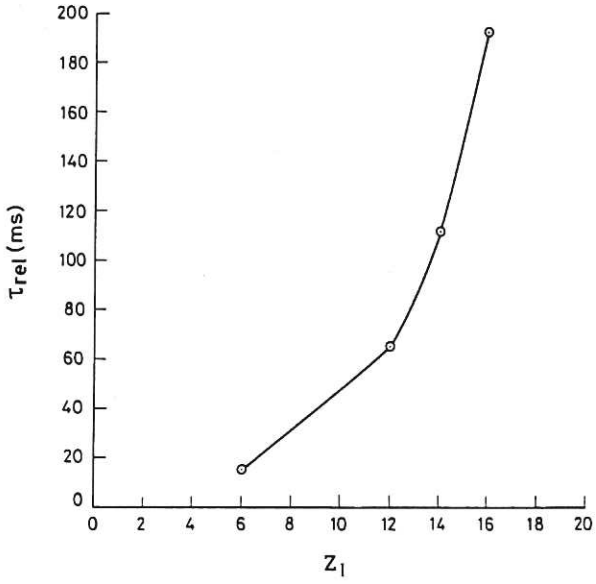

Fig.9. Scaling of τ_{rel} with impurity Z_I as predicted by the model.